

Heat Capacities and Excess Enthalpies of 1-Ethyl-3-methylimidazolium-Based Ionic Liquids and Water

Lindsay E. Ficke, Héctor Rodríguez,[†] and Joan F. Brennecke*

Department of Chemical and Biomolecular Engineering, University of Notre Dame, 182 Fitzpatrick Hall, Notre Dame, Indiana 46556

Heat capacities and excess enthalpies were determined for three different binary water + ionic liquid systems, from (283.15 to 348.15) K, and covering the entire composition range. Specifically, the three completely water-miscible ionic liquids used were 1-ethyl-3-methylimidazolium ethylsulfate, 1-ethyl-3-methylimidazolium trifluoromethanesulfonate, and 1-ethyl-3-methylimidazolium trifluoroacetate. The influence of temperature and composition was assessed, and suitable equations were used to correlate the experimental data. In addition, it was found that 1-ethyl-3-methylimidazolium ethylsulfate decomposes in the presence of water to form 1-ethyl-3-methylimidazolium hydrogen sulfate and ethanol under ambient conditions.

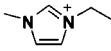
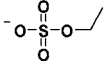
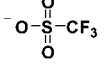
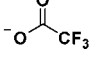
Introduction

Ionic liquids (ILs) are a family of low melting salts which have generated burgeoning interest in industry and academia over the past decade. The appealing set of properties exhibited by these salts, which are liquid at or near room temperature, suggests the possible use of ILs in a wide variety of applications.¹ Since many ILs are entirely miscible with water, the use of water + IL mixtures as working fluids in processes is possible. Introducing an IL as a replacement may improve the efficiency or decrease the environmental impact of conventional processes involving aqueous solutions of salts or other soluble substances. An example of particular interest is absorption refrigeration.

The development of practical processes involving water + IL systems will require basic thermodynamic data, which are generally lacking for water + IL systems. For thermal applications, one of the properties of interest is the heat capacity. To date, several publications have reported experimental values of heat capacity for pure ILs as a function of temperature.^{2–24} However, there are only a few papers reporting heat capacities of a binary mixture including water + IL (1-butyl-3-methylimidazolium tetrafluoroborate, [bmim][BF₄], 1-butyl-3-methylpyridinium tetrafluoroborate, [bmpy][BF₄], and 1-butyl-3-methylimidazolium tosylate, [bmim][Tos]).^{6,20,21}

The excess enthalpy is another fundamental property for which literature data for water + IL mixtures over the entire composition range and at multiple temperatures are sparse. Several groups have reported the excess enthalpies at very low composition ranges and room temperature for water + tetrafluoroborate (BF₄[−]), + chloride (Cl[−]), + bis(trifluoromethylsulfonyl)imide ([Tf₂N][−]), and + ammonioacetate ([Gly][−]) based ILs.^{11,25–30} Constantinescu et al. have reported exothermic excess enthalpies for water + two ILs ([choline][lactate] and [choline][glycolate]) over the entire composition range and temperatures of (303.15, 315.15, and 323.15) K.³¹ Ortega et al. reported

Table 1. IL Structures and Abbreviations

Ion	Abbreviation	Name
	[emim]	1-ethyl-3-methylimidazolium
	[EtSO ₄]	Ethylsulfate
	[OTf]	Trifluoromethanesulfonate or Triflate
	[TFA]	Trifluoroacetate

exothermic enthalpies of mixing for water + [bmpy][BF₄] over the entire composition range at (298.15 and 318.15) K.³² Rebelo et al. have reported endothermic excess enthalpy values for water + [bmim][BF₄] over the entire composition range from (278.15 to 333.15) K.⁶ Katayanagi et al. reported excess partial molar enthalpies for water + two ILs ([bmim][BF₄] and 1-butyl-3-methylimidazolium iodide, [bmim][I]) over the entire composition range at 198.15 K.³³ No excess enthalpy data have been reported for the systems investigated in this study.

In this work, heat capacities and excess enthalpies are reported for binary systems of water and three different hydrophilic and noncorrosive ILs, with melting points below that of water: 1-ethyl-3-methylimidazolium ethylsulfate, [emim][EtSO₄]; 1-ethyl-3-methylimidazolium trifluoromethanesulfonate (or triflate), [emim][OTf]; and 1-ethyl-3-methylimidazolium trifluoroacetate, [emim][TFA]. The structures and abbreviations of the ILs are shown in Table 1. In addition to the characteristics aforementioned, these ILs were selected because they were believed to be more chemically stable than some other ILs,^{25,34} they have relatively low viscosities,³⁵ and they have a common cation.

The experimental determinations of heat capacity and excess enthalpy for the systems water + [emim][EtSO₄], water + [emim][OTf], and water + [emim][TFA] covered the entire composition range and a wide temperature range, from (283.15 to 348.15) K.

* Corresponding author. Telephone: (574)631-5847. Fax: (574)631-8366. E-mail: jfb@nd.edu.

[†] Current Address: The QUILL Centre, School of Chemistry and Chemical Engineering, The Queen's University of Belfast, Belfast, BT9 5AG, Northern Ireland, U.K.

Experimental

Chemicals. The ILs used in the heat capacity experiments were synthesized in our laboratory. The structures of the final products were checked by nuclear magnetic resonance (NMR) spectroscopy.

The IL [emim][EtSO₄] was synthesized by direct reaction of equimolar amounts of 1-methylimidazole (Aldrich, 99 %, freshly redistilled over KOH) and diethylsulfate (Aldrich, 98 %),³⁶ adding the latter dropwise to the 1-methylimidazole in a round-bottomed flask, placed in an ice bath to keep the temperature low. Removal of any unreacted starting material was carried out by rotary evaporation and heating under high vacuum (<67 Pa) for two days. The water mass fraction of the final product was $69 \cdot 10^{-6}$, measured by Karl Fischer titration with a Metrohm 831 KF Coulometer.

In a similar way, ethyltrifluoromethanesulfonate (Aldrich, 99 %) and 1-methylimidazole were reacted at low temperature in a stirred round-bottomed flask with a reflux condenser, in the absence of any solvent, to form [emim][OTf]. A similar procedure can be found in the literature.³⁷ Unreacted starting materials were removed by heating under reduced pressure. The water mass fraction of the final liquid was found to be $44 \cdot 10^{-6}$, measured by Karl Fischer titration.

The procedure for the synthesis of [emim][TFA] was similar to that reported elsewhere.³⁷ Equimolar amounts of 1-ethyl-3-methylimidazolium bromide (Fluka, 97.0 %), further purified in our laboratory prior to use, and silver trifluoroacetate (Aldrich, 98 %), used as received, were dissolved in water. Both solutions were mixed and allowed to react for 24 h in a setup similar to that described for the synthesis of [emim][OTf]. The resulting solution was filtered to remove the AgBr precipitate, and water was partially removed in a rotary evaporator. The presence of bromide and silver ions in the product was tested by addition of AgNO₃ and NaCl solutions to probe vials containing aliquots of the reaction product. According to the precipitates observed in the tests, an additional amount of one of the starting materials was added to neutralize the excess of the other. The reaction and subsequent steps were repeated until no precipitate was observed in either of the tests, indicating bromide and silver mass fractions less than $1 \cdot 10^{-3}$. The purification was completed by drying the IL thoroughly under high vacuum at moderate temperature for several days. A water mass fraction of $678 \cdot 10^{-6}$ was assessed by Karl Fischer titration.

The ILs used for the excess enthalpy measurements were purchased from Solvent Innovations ([emim][EtSO₄] and [emim]-[OTf]) and Merck KGaA ([emim][TFA]), all of which had a purity of > 99 %, and the samples were used as received except for drying. The average water mass fraction for the ILs was $(152, 157, \text{ and } 64) \cdot 10^{-6}$, respectively. High-purity water, deionized through a Milli-Q Water System, was used for all the experiments.

Heat Capacity Measurements. Heat capacity measurements were performed for all three water + IL mixtures over a range of temperatures and compositions. The mixtures were prepared by mass using a Mettler Toledo AE 160 balance, precise to within $\pm 1 \cdot 10^{-4}$ g. Good mixing was ensured by magnetic stirring. A sample of ca. (20 to 40) mg was placed in an aluminum pan, covered with a lid of the same material, and hermetically sealed. All the samples were prepared immediately prior to performing the measurements to avoid variations in composition due to evaporation or sorption of water.

Measurements were performed in a differential scanning calorimeter (DSC), manufactured by Mettler-Toledo, model DSC822^e, with STAR^e software data collection. Heat capacities

were determined by the sapphire method, extensively used in the literature and particularly with ILs.^{3,5,7-10,14,22} This method is based on the comparison of the DSC signal of the sample with the DSC signal of a calibration sample of known heat capacity (sapphire). Both curves must be blank corrected. Therefore, for each measurement, a minimum of three runs were carried out: the blank, with an empty crucible; the sapphire; and the sample itself. In addition, a cleaning process at 600 °C for 10 min, followed by one or two extra blank curves to condition the measuring cell, was run prior to each of the measurement sequences. The uncertainty attained by the sapphire method is better than ± 3 %; however, taking into account the uncertainties in weighing involved, an overall uncertainty of ± 4 % is estimated for the values reported in this work.

The temperature program used for the blank, sapphire, and sample runs in the DSC included a 5 min 278.15 K isothermal stage, followed by a temperature ramp from (278.15 to 348.15) K at a rate of $10 \text{ K} \cdot \text{min}^{-1}$ and a final 5 min isothermal segment at 348.15 K. From this data, heat capacity values were calculated at every 5 K between (283.15 and 343.15) K.

The method was tested for water, and the results were found to be in good agreement, within the experimental error, with values in reference literature.³⁸

Excess Enthalpy Measurements. Excess enthalpies of water + IL were obtained by calorimetry, using a Setaram C80 calorimeter. A DSC measures the heat flow to or from the sample vessel compared to an empty reference vessel, as the result of a chemical reaction, change of state, or mixing. The temperatures of the vessels are maintained at the same temperature of the calorimetric block by Peltier elements. The calorimeter used here has high accuracy due to three-dimensional heat flow transducers completely surrounding the experimental vessels.

The stainless steel C80 mixing vessels were dried in an oven at 388.15 K prior to sample preparation. Water was placed in the bottom portion of the vessel and IL in the top. The mixing occurred using continuous reversal which consisted of rotating the entire vessel 180°. The bottom section of the vessel had a stainless steel lid that fell off with the 180° turn and served as a “stirrer”. In addition, mercury was used to completely separate the two liquids prior to mixing.

The ILs were saturated with mercury prior to the experiments by mixing for 22 h at 323.15 K. The mass fraction of mercury which dissolved or remained suspended in the IL was less than $50 \cdot 10^{-6}$, which was confirmed by analysis with inductively coupled plasma optical emission spectroscopy (ICP-OES). In addition, the difference in the excess enthalpies of the mercury saturated IL and a clean IL was small and within the experimental error.

The measurements were performed at atmospheric pressure including temperatures from (313.15 to 348.15) K and over the entire range of mole fraction (0.25, 0.50, and 0.75) as determined by mass. The vessels were loaded in a dry nitrogen environment using a Mettler Toledo XS205DU analytical balance accurate to $\pm 1 \cdot 10^{-5}$ g. The water content of the ILs was measured by Karl Fischer titration.

The method included three segments: a dynamic segment ramping up to the desired temperature; a three hour isotherm prior to mixing followed by a one hour isotherm after mixing; and a dynamic segment ramping down to room temperature. The mixing itself occurred for 69 s.

The experimental uncertainty associated with this method is estimated to be 2 % considering the propagation of error and the ability to reproduce measurements with different samples

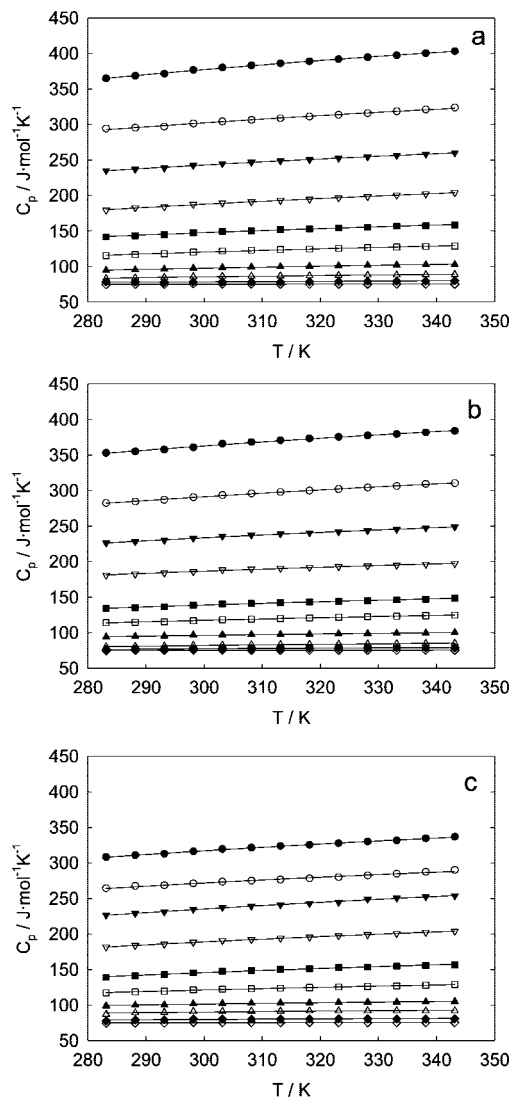


Figure 1. Molar heat capacity, C_p , for the binary systems water (1) + IL (2) as a function of temperature, at different approximate mass fractions of water: ●, 0 %; ○, 2 %; ▼, 5 %; ▽, 10 %; ■, 20 %; □, 30 %; ▲, 50 %; △, 70 %; ◆, 90 %; ◇, 100 %. Empirical correlations are plotted as solid lines. ILs: (a) [emim][EtSO₄]; (b) [emim][OTf]; (c) [emim][TFA].

over time. The method was verified using organic + organic systems (i.e., benzene + cyclohexane, 1-propanol + propyl acetate, and pyridine + acetic acid) at the extreme temperatures, both (313.15 and 348.15) K, which produced results in agreement with the literature and within the experimental uncertainty.³⁹

Results and Discussion

Heat Capacity: Effect of Temperature. Molar heat capacities for water + IL systems, from pure IL to pure water, are plotted in Figure 1 as a function of temperature. The experimental data can be found in Tables S1 to S3 of the Supporting Information. A slight increase of C_p with increasing temperature is observed for IL-rich compositions, which diminishes for water-rich samples. From Figure 1, it is clear that the C_p of the pure ILs is much greater than that of water. This is not surprising, since C_p is related to the number of translational, vibrational, and rotational energy storage modes in the molecule,⁷ and the molecular weight of the ILs is much greater than water. The heat capacity of the mixtures decreases with increasing water mole fraction. Our measurements of the pure IL heat capacities

Table 2. Fit Parameters a and b , Equation 1, and Standard Deviation, σ , for the Empirical Correlation of Molar Heat Capacity in Binary Systems Water (1) + IL (2) as a Function of Temperature, in the Range from (283.15 to 343.15) K

x_1	$a/10^2 \text{ J}\cdot\text{mol}^{-1}\cdot\text{K}^{-1}$	$b/10^4 \text{ J}\cdot\text{mol}^{-1}$	$\sigma/\text{J}\cdot\text{mol}^{-1}\cdot\text{K}^{-1}$
Water + [emim][EtSO ₄]			
0.0000	5.827	-6.161	0.5
0.2120	4.656	-4.899	0.8
0.4079	3.792	-4.087	0.4
0.5925	3.164	-3.862	0.4
0.7660	2.390	-2.740	0.5
0.8495	1.929	-2.178	0.5
0.9282	1.433	-1.368	0.3
0.9684	1.150	-0.888	0.4
0.9916	0.886	-0.303	0.3
1.0000	0.783	-0.096	0.2
Water + [emim][OTf]			
0.0000	5.351	-5.166	0.8
0.2259	4.454	-4.622	0.5
0.4351	3.553	-3.651	0.5
0.6152	2.745	-2.636	0.5
0.7835	2.146	-2.270	0.3
0.8614	1.771	-1.789	0.3
0.9353	1.274	-0.931	0.3
0.9712	1.086	-0.796	0.2
0.9924	0.926	-0.458	0.3
1.0000	0.783	-0.096	0.2
Water + [emim][TFA]			
0.0000	4.699	-4.583	0.5
0.2025	4.021	-3.907	0.9
0.3973	3.846	-4.480	0.7
0.5817	3.089	-3.600	0.3
0.7562	2.396	-2.819	0.7
0.8420	1.818	-1.816	0.3
0.9256	1.326	-0.935	0.3
0.9668	1.114	-0.636	0.8
0.9912	0.914	-0.346	0.5
1.0000	0.783	-0.096	0.2

for [emim][OTf] and [emim][EtSO₄] agree with those reported by Diedrichs and Gmehling¹⁴ and Zhang et al.¹⁸ within experimental uncertainty. Fernández et al.¹⁹ reported a heat capacity of [emim][EtSO₄] at 298.15 K (421.1 J·mol⁻¹·K⁻¹) which is higher than the values obtained in both this study and by Zhang et al.¹⁸ [(377 and 378) J·mol⁻¹·K⁻¹, respectively]. This can be attributed to the purity (Sigma-Aldrich ≥ 95 %) and high water mass fraction ($2\cdot 10^{-3}$) of the IL used by Fernández et al.¹⁹

Most correlations of experimental heat capacity data as a function of temperature in the literature consist of empirical polynomial equations (often just straight lines).^{2,3,6-10,13,22} For the three binary systems in this work, we found excellent fit to the experimental data with the following equation

$$C_p = a + \frac{b}{T} \quad (1)$$

where T is the absolute temperature and a and b are the fit parameters. This equation has been used previously to correlate this type of data for pure ILs.¹⁴ Least-squares fits led to the values summarized in Table 2. The low values of the corresponding standard deviations, σ , also shown in Table 2, confirm the ability of the proposed equation to provide a good correlation of the experimental data, with only two adjusting parameters. Although the lowest standard deviations are for pure water, this is because the absolute value of C_p is the lowest for pure water. The empirical correlation presented here is not intended to provide an accurate description of C_p of pure water itself but just a suitable correlation for the binary systems water + IL throughout the

Table 3. Specific Heat Capacities (c_p) of the Pure ILs at Selected Temperatures

T/K	$c_p/J \cdot g^{-1} \cdot K^{-1}$		
	[emim][EtSO ₄]	[emim][OTf]	[emim][TFA]
283.15	1.54	1.36	1.37
293.15	1.57	1.37	1.40
303.15	1.61	1.41	1.43
313.15	1.63	1.42	1.44
323.15	1.66	1.44	1.46
333.15	1.68	1.46	1.48
343.15	1.71	1.48	1.50

whole compositional spectrum. The resulting correlations are plotted with solid lines in Figure 1.

In Table 3, the specific heat capacities, c_p , are shown for the three pure ILs over the temperature range studied. The c_p values for ILs are much lower than those for water, $4.18 J \cdot g^{-1} \cdot K^{-1}$ at 293.15 K.⁴⁰ This means less energy will be required to produce a certain temperature increase in a given mass of IL than in the same mass of water.

The relative value of the heat capacities of the IL changes depending on whether a mole or mass basis is considered. Of the three ILs studied, the C_p values are highest for [emim]-[EtSO₄], followed closely by [emim][OTf], but [emim][TFA] is significantly lower. [emim][EtSO₄] also has the highest c_p values, but [emim][OTf] and [emim][TFA] have very similar c_p values over the temperature range studied.

Heat Capacity: Effect of Composition. The variation of C_p with composition is shown in Figure 2 for the highest and lowest isotherms of the three water + IL binary systems. As expected, C_p decreases with increasing mole fraction of water in the mixture. The excess molar heat capacity, C_p^E , is the difference between the mixture heat capacity and the pure components

$$C_p^E = C_p - \sum x_i \cdot C_{p,i} \quad (2)$$

where C_p is the molar heat capacity of the mixture; $C_{p,i}$ is the molar heat capacity of the pure compound; and x_i is its mole fraction. The values of C_p^E for the three systems studied here are very small, on the same order of magnitude as the experimental uncertainty, so no significant analysis can be carried out. This means that an assumption of a linear decrease of C_p with the concentration of water (i.e., $C_p^E \approx 0$) is a very good estimate. In Table 4, the parameters corresponding to the linear fit of the isotherms of C_p as a function of mole fraction of water are shown for the three binary systems studied. The linear correlations for the highest and the lowest experimental temperature are plotted as the solid lines in Figure 2. The experimental points do not lay far from the straight lines, consistent with the low values of standard deviation listed in Table 4.

Excess Enthalpy. The excess molar enthalpies, H^E , of the three water + IL mixtures, [emim][EtSO₄], [emim][OTf], and [emim][TFA], are shown in Figure 3a, b, and c, respectively, at temperatures (313.15, 323.15, 333.15, and 348.15) K. The experimental data were fit to a Redlich–Kister-type equation as represented by the solid lines

$$H^E = x_1 \cdot x_2 (A + B(x_1 - x_2) + C(x_1 - x_2)^2) \quad (3)$$

where x_i is the mole fraction of component i and A , B , and C are the fitting parameters. The parameters A , B , and C , along with the standard deviations, σ , are shown in Table 5. The experimental data can be found in Tables S4 to S6 in the Supporting Information.

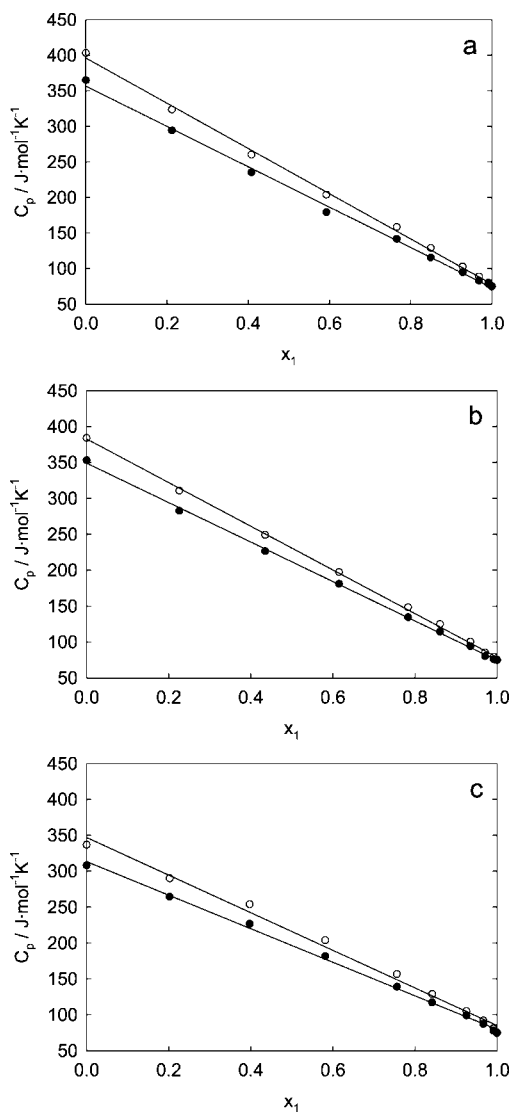


Figure 2. Molar heat capacity, C_p , for the binary systems water (1) + IL (2) as a function of mole fraction of water, at different temperatures: ●, 283.15 K; ○, 343.15 K. Linear fits are plotted as solid lines. ILs: (a) [emim][EtSO₄]; (b) [emim][OTf]; (c) [emim][TFA].

The water + [emim][EtSO₄] mixture (Figure 3a) is exothermic. These negative values of the excess enthalpy suggest that the water/IL interactions are stronger than the corresponding IL/IL and water/water interactions. It is important to note that at the lower composition the excess enthalpy decreases with increasing temperature and at the higher composition the excess enthalpy increases with increasing temperature. The experimental uncertainty of the measurements is 2 %; therefore, the change in the temperature trend is real and is not within experimental uncertainty.

The consistency of the excess enthalpies with the excess heat capacities cannot be checked because, as mentioned previously, the experimental uncertainty for the heat capacity measurements is of the same order of magnitude as the excess heat capacities.

The excess enthalpy is endothermic for the water + [emim][OTf] mixture (Figure 3b), and the excess enthalpy increases with increasing temperature. The water + [emim][TFA] mixture (Figure 3c) is exothermic, and again, the temperature trend shows that the excess enthalpy increases with increasing temperature.

For the system of water + [emim][TFA], Domanska et al. calculated an infinite dilution partial molar enthalpy of water

Table 4. Slope, a , and Intercept, b , Along with the Standard Deviation, σ , for the Correlation of Molar Heat Capacity in Binary Systems Water + IL as a Function of Mole Fraction of Water

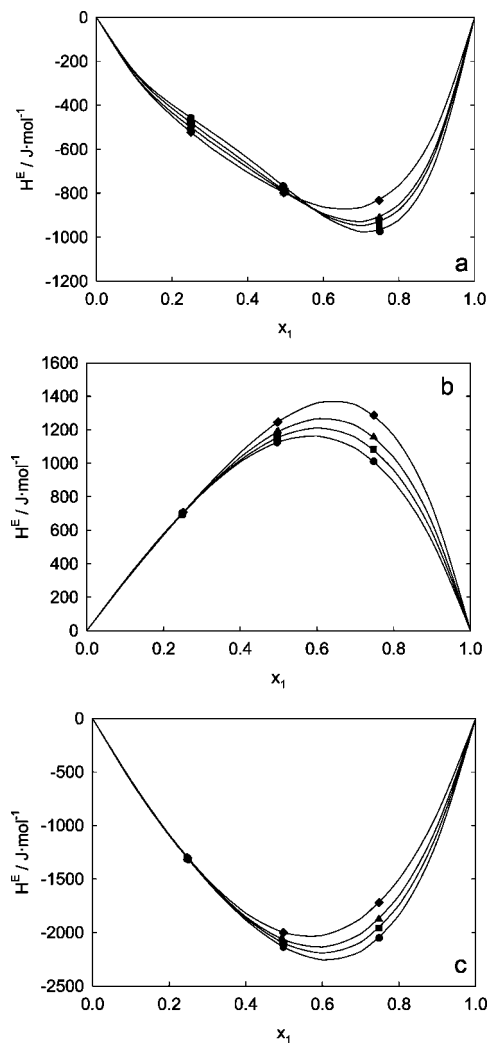
T/K	$a/10^2 \text{ J}\cdot\text{mol}^{-1}\cdot\text{K}^{-1}$	$b/10^2 \text{ J}\cdot\text{mol}^{-1}\cdot\text{K}^{-1}$	$\sigma/\text{J}\cdot\text{mol}^{-1}\cdot\text{K}^{-1}$
Water + [emim][EtSO ₄]			
283.15	-2.836	3.566	5.1
288.15	-2.862	3.599	5.0
293.15	-2.883	3.625	5.1
298.15	-2.927	3.680	5.1
303.15	-2.960	3.717	5.0
308.15	-2.987	3.747	5.0
313.15	-3.015	3.778	5.0
318.15	-3.041	3.808	5.0
323.15	-3.068	3.838	5.1
328.15	-3.094	3.868	5.0
333.15	-3.121	3.899	5.0
338.15	-3.149	3.929	4.9
343.15	-3.180	3.961	4.8
Water + [emim][OTf]			
283.15	-2.745	3.489	2.7
288.15	-2.763	3.512	2.7
293.15	-2.789	3.541	2.5
298.15	-2.816	3.579	2.3
303.15	-2.862	3.628	2.7
308.15	-2.885	3.653	2.6
313.15	-2.908	3.679	2.7
318.15	-2.932	3.705	2.8
323.15	-2.953	3.729	2.9
328.15	-2.975	3.754	2.9
333.15	-2.994	3.776	2.9
338.15	-3.021	3.805	2.8
343.15	-3.038	3.826	3.0
Water + [emim][TFA]			
283.15	-2.336	3.133	4.1
288.15	-2.357	3.165	4.3
293.15	-2.372	3.186	4.8
298.15	-2.396	3.223	5.3
303.15	-2.429	3.259	5.7
308.15	-2.448	3.282	6.1
313.15	-2.468	3.305	6.4
318.15	-2.487	3.327	6.8
323.15	-2.509	3.352	7.0
328.15	-2.541	3.386	7.7
333.15	-2.561	3.408	7.9
338.15	-2.592	3.440	8.0
343.15	-2.618	3.468	8.1

to be $-5607 \text{ J}\cdot\text{mol}^{-1}$ which was obtained from infinite dilution activity coefficients at temperatures of (348.15, 358.15, and 368.15) K.⁴¹ Using the experimental data from this study at 348.15 K (the lower end of temperature for Domanska et al.), the calculated partial molar enthalpy of water at a mole fraction of 0.001 is $-6020 \text{ J}\cdot\text{mol}^{-1}$. This is in very good agreement as the partial molar enthalpy for this system increases with increasing temperature.

The excess enthalpies for all three of these systems are very small, with the maximums at $\pm (1 \text{ to } 2) \text{ kJ}\cdot\text{mol}^{-1}$. Therefore, as a first approximation, one may be able to neglect H^E in calculating enthalpies for these mixtures. For example, to calculate the enthalpy of the water + IL liquid mixture at a temperature T relative to a reference temperature by eq 4, one finds that the first two terms are large in comparison to the excess enthalpy.

$$H_f = \left(\int_{273}^T C_p dT \right)_{\text{H}_2\text{O}} \frac{n_{\text{H}_2\text{O}}}{n_{\text{total}}} + \left(\int_{273}^T C_p dT \right)_{\text{IL}} \frac{n_{\text{IL}}}{n_{\text{total}}} + H^E \quad (4)$$

Nonetheless, the excess enthalpies can provide a starting point for understanding species interactions. The excess enthalpy can be best explained as the difference in the strength of interactions between unlike species compared to like species. Here we use

**Figure 3.** Excess enthalpy, H^E , for the binary systems water (1) + IL (2) as a function of mole fraction of water, at different temperatures: ●, 313.15 K; ■, 323.15 K; ▲, 333.15 K; ◆, 348.15 K. Empirical correlations are plotted as solid lines. ILs: (a) [emim][EtSO₄]; (b) [emim][OTf]; (c) [emim][TFA].**Table 5.** Constants A , B , and C , along with the Standard Deviation, σ , for the Correlation of Excess Enthalpy in Binary Systems Water + IL as a Function of Mole Fraction of Water, Equation 3

T/K	$A/10^3 \text{ J}\cdot\text{mol}^{-1}$	$B/10^3 \text{ J}\cdot\text{mol}^{-1}$	$C/10^2 \text{ J}\cdot\text{mol}^{-1}$	$\sigma/\text{J}\cdot\text{mol}^{-1}$
Water + [emim][EtSO ₄]				
313.14	-3.104	-2.732	-28.28	3.29
323.12	-3.169	-2.407	-23.99	9.69
333.11	-3.193	-2.175	-22.87	5.48
348.12	-3.203	-1.635	-16.41	1.44
Water + [emim][OTf]				
313.13	4.512	1.609	2.030	0.80
323.12	4.625	2.003	4.508	0.76
333.13	4.764	2.400	7.270	0.55
348.12	5.000	3.095	11.79	0.71
Water + [emim][TFA]				
313.04	-8.561	-3.873	-16.45	0.52
323.04	-8.411	-3.387	-12.29	0.61
333.06	-8.284	-2.930	-8.225	0.91
348.06	-8.011	-2.172	-1.854	0.80

the acid dissociation constant, a measure of unlike species interactions, and the glass transition temperature, a measure of the strength of IL/IL interactions, to discuss the results.

The pK_a , the acid dissociation constant, is an indicator of the strength of the conjugate base of an acid. In our case, it is a

Table 6. Acid Dissociation Constants for the Conjugate Acids of the IL Anions Used in This Work

Acid	Structure	pK _a
Trifluoromethanesulfonic		-11 ⁴²
Ethylsulfuric		-3.14 ⁴³
Trifluoroacetic		0.52 ⁴⁴

measure of the strength of the basicity of the anion. A stronger base should have greater interactions with water; therefore, a large pK_a corresponds to a strong base and strong anion–water interactions. The pK_a's of the acids of interest are shown in Table 6. The pK_a of trifluoromethanesulfonic acid is -11,⁴² indicating that it should have weak interactions with water, which is consistent with the experimental endothermic excess enthalpy ($H^E < 1373 \text{ J}\cdot\text{mol}^{-1}$). The ethylsulfuric acid has a larger pK_a of -3.14,⁴³ indicating stronger interactions with water than [emim][OTf], and this is consistent with the slightly exothermic excess enthalpy for water + [emim][EtSO₄] ($H^E > -979 \text{ J}\cdot\text{mol}^{-1}$). Lastly, the trifluoroacetic acid has the largest pK_a of 0.52,⁴⁴ making the [TFA]⁻ anion the strongest base of the three. This suggests that [emim][TFA] should have the strongest interactions with water. Indeed, water + [emim][TFA] has the largest exothermic excess enthalpy of the systems studied ($H^E > -2258 \text{ J}\cdot\text{mol}^{-1}$).

The pK_a's indicate the strength of the anion–water interactions. The [emim][OTf] has the weakest anion–water interactions, and [emim][TFA] has the strongest anion–water interactions. Therefore, the pK_a's aptly explain the excess enthalpies for these three systems. However, there are other examples in the literature which do not follow this trend.

Constantinescu et al. reported the excess enthalpies of both [choline][lactate] and [choline][glycolate] with water.³¹ The structures of the respective acids are very similar, and the pK_a's are virtually the same;^{44,45} however, the excess enthalpies are very different. For a given isotherm, there is an order of magnitude difference between the excess enthalpies despite the similar pK_a's. Therefore, the interactions in water + IL systems cannot be explained solely by the pK_a's of the conjugate acids of the anions.

The glass transition temperature is the temperature below which an amorphous material acts as a solid and above which it acts as a liquid. This temperature can indicate the strength of the cation–anion interactions in a pure IL and, thus, is an indicator of the strength of IL/IL interactions. An IL with strong cation–anion interactions should have a high glass transition temperature. The glass transition temperature can be measured on a DSC.

For similar unlike pair interactions (IL/water), the IL with stronger IL/IL interactions should have a larger (larger positive value or smaller negative value) excess enthalpy. The glass transition temperature of [emim][EtSO₄] has been reported as 192.85 K.¹⁸ On the basis of the excess enthalpies, we would then expect the glass transition temperature of [emim][OTf] to be higher and the [emim][TFA] to be lower than that of [emim][EtSO₄]. DSC measurements, using a ramp rate of 10 °C·min⁻¹, of [emim][OTf] and [emim][TFA] confirm this trend (Table 7). The glass transition temperature of [emim][TFA] is 182 K, which indicates weaker cation–anion interactions than in [emim][EtSO₄]. [emim][OTf] does not have a glass transition temperature but melts at 259 K. This suggests strong interactions between the anion and cation for [emim][OTf]. Thus, the glass transition temperatures, indicating

Table 7. Glass Transition Temperatures of the Pure ILs

IL	T _g /K
[emim][OTf]	259 ^a
[emim][EtSO ₄]	192.85 ¹⁸
[emim][TFA]	182

^a Melting point.

the strength of IL/IL interactions, are also consistent with the observed trends in excess enthalpies.

Decomposition of [emim][EtSO₄]. It is of great importance to note that the IL [emim][EtSO₄] was found to decompose over time by reacting with water to form 1-ethyl-3-methylimidazolium hydrogen sulfate, [emim][HSO₄], and ethanol. This was discovered when checking the batch to batch consistency of the ILs. The batch used in this study was compared to two other batches: a commercial sample from 2004 and a batch made in-house in 2006. A triple quadrupole liquid chromatography–mass spectrometry (LCMS) apparatus confirmed the decomposition products. Quantitatively, NMR spectroscopy revealed that the 2004 and 2006 batches were approximately 23 % and 28 % decomposed, respectively, even though these samples had been dried before storage. The decomposition of the batch of [emim][EtSO₄] used in this study was below the detection limit of the instrument (< 1 % decomposed). The NMR results can be found in Figure S1 of the Supporting Information. Clearly, decomposition must be taken into account when trying to reproduce any physical property data with this IL. Due to the composition and property changes with time, [emim]-[EtSO₄] may not be a good IL choice for practical applications.

Conclusions

Heat capacities for the binary systems water + [emim]-[EtSO₄], water + [emim][OTf], and water + [emim][TFA] were experimentally determined in the temperature range from (283.15 to 343.15) K and over the whole range of composition. The molar heat capacities (C_p) decreased as the water concentration increased, with the C_p of the pure ILs being 4 to 5 times greater than that of water. A slight increase of C_p with increasing temperature was observed. Since the molecular weights of the ILs are high, the specific heat capacity (c_p) of water is much higher than that of the pure ILs. The variation of C_p with temperature was correlated with a two-parameter empirical equation; for the correlation of C_p as a function of mole fraction, a straight line was adequate.

The excess enthalpies were positive values (endothermic) for water + [emim][OTf] and negative values (exothermic) for water + [emim][EtSO₄] and water + [emim][TFA]. The H^E values were fit with a Redlich–Kister-type equation using three fitting parameters. The excess enthalpy measurements provide insight into the interactions of the species in solution, which is important for gaining a fundamental thermodynamic understanding, selecting ILs for processes, and predicting the effect of water as an impurity.

In addition, these experimental measurements showed that [emim][EtSO₄] decomposes in the presence of water under ambient conditions.

Acknowledgment

We thank Dennis Birdsell and Michelle Joyce of the Center for Environmental Science & Technology at the University of Notre Dame for their expertise in optical emission and mass spectrometry,

respectively. Lastly, we are grateful to Alexandre Chapeaux for his help with the NMR spectroscopy.

Supporting Information Available:

Experimental molar heat capacities of the systems water + IL (Table S1 to S3); experimental excess enthalpies of the systems water + IL (Tables S4 to S6); and NMR results of the [emim][EtSO₄] decomposition (Figure S1). This material is available free of charge via the Internet at <http://pubs.acs.org>.

Literature Cited

- Rogers, R. D.; Seddon, K. R., Eds. *Ionic Liquids IIIB: Fundamentals, Progress, Challenges, and Opportunities: Transformations and Processes*; ACS Symposium Series: Washington, DC, 2005, Vol. 902.
- Holbrey, J. D.; Reichert, W. M.; Reddy, R. G.; Rogers, R. D. Heat Capacities of Ionic Liquids and Their Applications as Thermal Fluids. In *Ionic Liquids as Green Solvents*; Rogers, R. D., Seddon, K. R., Eds.; ACS Symposium Series: Washington, DC, 2003, Vol. 856.
- Fredlake, C. P.; Crosthwaite, J. M.; Hert, D. G.; Aki, S. N. V. K.; Brennecke, J. F. Thermophysical Properties of Imidazolium-Based Ionic Liquids. *J. Chem. Eng. Data* **2004**, *49*, 954–964.
- Kabo, G. J.; Blokhin, A. V.; Paulechka, Y. U.; Kabo, A. G.; Shymanovich, M. P. Thermodynamic Properties of 1-Butyl-3-methylimidazolium Hexafluorophosphate in the condensed State. *J. Chem. Eng. Data* **2004**, *49*, 453–461.
- Kim, K.-S.; Shin, B.-K.; Lee, H.; Ziegler, F. Refractive index and heat capacity of 1-butyl-3-methylimidazolium bromide and 1-butyl-3-methylimidazolium tetrafluoroborate, and vapor pressure of binary systems for 1-butyl-3-methylimidazolium bromide + trifluoroethanol and 1-butyl-3-methylimidazolium tetrafluoroborate + trifluoroethanol. *Fluid Phase Equilib.* **2004**, *218*, 215–220.
- Rebelo, L. P. N.; Najdanovic-Visak, V.; Visak, Z. P.; Nunes da Ponte, M.; Szydłowski, J.; Cerdeiriña, C. A.; Troncoso, J.; Román, L.; Esperança, J. M. S. S.; Guedes, H. J. R.; de Sousa, H. C. A detailed thermodynamic analysis of [C₄mim][BF₄] + water as a case study to model ionic liquid aqueous solutions. *Green Chem.* **2004**, *6*, 369–381.
- Crosthwaite, J. M.; Muldoon, M. J.; Dixon, J. K.; Anderson, J. L.; Brennecke, J. F. Phase transition and decomposition temperatures, heat capacities and viscosities of pyridinium ionic liquids. *J. Chem. Thermodyn.* **2005**, *37*, 559–568.
- Domańska, U.; Bogel-Łukasik, R. Physicochemical Properties and Solubility of Alkyl-(2-hydroxyethyl)-dimethylammonium Bromide. *J. Phys. Chem. B* **2005**, *109*, 12124–12132.
- Du, Z.; Li, Z.; Guo, S.; Zhang, J.; Zhu, L.; Deng, Y. Investigation of Physicochemical Properties of Lactam-Based Brønsted Acidic Ionic Liquids. *J. Phys. Chem. B* **2005**, *109*, 19542–19546.
- Van Valkenburg, M. E.; Vaughn, R. L.; Williams, M.; Wilkes, J. S. Thermochemistry of ionic liquid heat-transfer fluids. *Thermochim. Acta* **2005**, *425*, 181–188.
- Waliszewski, D.; Stępnik, I.; Piekarski, H.; Lewandowski, A. Heat capacities of ionic liquids and their heats of solution in molecular liquids. *Thermochim. Acta* **2005**, *433*, 149–152.
- Blokhin, A. V.; Paulechka, Y. U.; Kabo, G. J. Formation of metastable crystals of [C₄mim][NTf₂] and [C₆mim][NTf₂]. *Thermochim. Acta* **2006**, *445*, 75–77.
- Blokhin, A. V.; Paulechka, Y. U.; Kabo, G. J. Thermodynamic Properties of [C₆mim][NTf₂] in the Condensed State. *J. Chem. Eng. Data* **2006**, *51*, 1377–1388.
- Diedrichs, A.; Gmehling, J. Measurement of heat capacities of ionic liquids by differential scanning calorimetry. *Fluid Phase Equilib.* **2006**, *244*, 68–77.
- Shimizu, Y.; Ohte, Y.; Yamamura, Y.; Saito, K.; Atake, T. Low-Temperature Heat Capacity of Room-Temperature Ionic Liquid, 1-Hexyl-3-methylimidazolium Bis(trifluoromethylsulfonyl)imide. *J. Phys. Chem. B* **2006**, *110*, 13970–13975.
- Troncoso, J.; Cerdeiriña, C. A.; Sanmamed, Y. A.; Román, L.; Rebelo, L. P. N. Thermodynamic Properties of Imidazolium-Based Ionic Liquids: Densities, Heat Capacities, and Enthalpies of Fusion of [bmim][PF₆] and [bmim][NTf₂]. *J. Chem. Eng. Data* **2006**, *51*, 1856–1859.
- Yamamoto, O.; Minamimoto, Y.; Inamura, Y.; Hayashi, S.; Hamaguchi, H. Heat capacity and glass transition of an ionic liquid 1-butyl-3-methylimidazolium chloride. *Chem. Phys. Lett.* **2006**, *423*, 371–375.
- Zhang, Z.-H.; Tan, Z.-C.; Sun, L.-X.; Jia-Zhen, Y.; Lv, X.-C.; Shi, Q. Thermodynamic investigation of room temperature ionic liquid: The heat capacity and standard enthalpy of formation of EMIES. *Thermochim. Acta* **2006**, *447* (2), 141–146.
- Fernández, A.; Torrecilla, J. S.; García, J.; Rodríguez, F. Thermophysical Properties of 1-Ethyl-3-methylimidazolium Ethylsulfate and 1-Butyl-3-methylimidazolium Methylsulfate Ionic Liquids. *J. Chem. Eng. Data* **2007**, *52*, 1979–1983.
- García-Miñaja, G.; Troncoso, J.; Román, L. Density and Heat Capacity as a Function of Temperature for Binary Mixtures of 1-Butyl-3-methylpyridinium Tetrafluoroborate + Water, + Ethanol, and + Nitromethane. *J. Chem. Eng. Data* **2007**, *52*, 2261–2265.
- Strechan, A. A.; Paulechka, Y. U.; Kabo, A. G.; Blokhin, A. V.; Kabo, G. J. 1-Butyl-3-methylimidazolium Tosylate Ionic Liquid: Heat Capacity, Thermal Stability, and Phase Equilibrium of Its Binary mixtures with Water and Caprolactam. *J. Chem. Eng. Data* **2007**, *52*, 1791–1799.
- Bandrés, I.; Giner, B.; Artigas, H.; Royo, F. M.; Lafuente, C. Thermophysical Comparative Study of Two Isomeric Pyridinium-Based Ionic Liquids. *J. Phys. Chem. B* **2008**, *112*, 3077–3084.
- Dávila, M. J.; Aparicio, S.; Alcalde, R.; García, B.; Leal, J. M. On the properties of 1-butyl-3-methylimidazolium octylsulfate ionic liquid. *Green Chem.* **2007**, *9*, 221–232.
- Blokhin, A. V.; Paulechka, Y. U.; Strechan, A. A.; Kabo, G. J. Physicochemical Properties, Structure, and Conformations of 1-Butyl-3-methylimidazolium Bis(trifluoromethanesulfonyl)imide [C₄mim]NTf₂ Ionic Liquid. *J. Phys. Chem. B* **2008**, *112*, 4357–4364.
- Archer, D. G.; Widegren, J. A.; Kirklín, D. R.; Magee, J. W. Enthalpy of solution of 1-octyl-3-methylimidazolium tetrafluoroborate in water and in aqueous sodium fluoride. *J. Chem. Eng. Data* **2005**, *50* (4), 1484–1491.
- Yang, J.-Z.; Zhang, Z.-H.; Fang, D.-W.; Li, J.-G.; Guan, W.; Tong, J. Studies on enthalpy of solution for ionic liquid: The system of 1-methyl-3-ethylimidazolium tetrafluoroborate (EMIBF₄). *Fluid Phase Equilib.* **2006**, *247*, 80–83.
- Guan, W.; Wang, H.; Li, L.; Zhang, Q.-G.; Yang, J.-Z. Enthalpy of solution of the ionic liquid BMIBF₄ in water. *Thermochim. Acta* **2005**, *437*, 196–197.
- Guan, W.; Yang, J.-Z.; Li, L.; Wang, H.; Zhang, Q.-G. Thermodynamic properties of aqueous solution containing ionic liquids 1. The heat of reaction mixed 1-methyl-3-butylimidazolium chloride with InCl₃. *Fluid Phase Equilib.* **2006**, *239* (2), 161–165.
- Fang, D.-W.; Sun, Y.-C.; Wang, Z.-W. Solution Enthalpies of Ionic Liquid 1-Hexyl-3-methylimidazolium Chloride. *J. Chem. Eng. Data* **2008**, *53*, 259–261.
- Zhang, Z.-F.; Li, J.-G.; Zhang, Q.-G.; Guan, W.; Yang, J.-Z. Enthalpy of Solution of Amino Acid Ionic Liquid 1-Ethyl-3-Methylimidazolium Ammonioacetate. *J. Chem. Eng. Data* **2008**, *53*, 1196–1198.
- Constantinescu, D.; Schaber, K.; Agel, F.; Klingele, M. H.; Schubert, T. J. S. Viscosities, vapor pressures, and excess enthalpies of choline lactate plus water, choline glycolate plus water, and choline methanesulfonate plus water systems. *J. Chem. Eng. Data* **2007**, *52* (4), 1280–1285.
- Ortega, J.; Vreekamp, R.; Marrero, E.; Penco, E. Thermodynamic Properties of 1-Butyl-3-methylpyridinium Tetrafluoroborate and Its Mixtures with Water and Alkanols. *J. Chem. Eng. Data* **2007**, *52*, 2269–2276.
- Katayanagi, H.; Nishikawa, K.; Shimozaki, H.; Miki, K.; Westh, P.; Koga, Y. Mixing Schemes in Ionic Liquid-H₂O Systems: A Thermodynamic Study. *J. Phys. Chem. B* **2004**, *108*, 19451–19457.
- Swatoski, R. P.; Holbrey, J. D.; Rogers, R. D. Ionic liquids are not always green: hydrolysis of 1-butyl-3-methylimidazolium hexafluorophosphate. *Green Chem.* **2003**, *5*, 361–363.
- Rodríguez, H.; Brennecke, J. F. Temperature and Composition Dependence of the Density and Viscosity of Binary Mixtures of Water + Ionic Liquid. *J. Chem. Eng. Data* **2006**, *51* (6), 2145–2155.
- Holbrey, J. D.; Reichert, W. M.; Swatoski, R. P.; Broker, G. A.; Pitner, W. R.; Seddon, K. R.; Rogers, R. D. Efficient, halide free synthesis of new, low cost ionic liquids: 1,3-dialkylimidazolium salts containing methyl- and ethyl-sulfate anions. *Green Chem.* **2002**, *4*, 407–413.
- Bonhôte, P.; Dias, A. P.; Armand, M.; Papageorgiou, N.; Kalyanasundaram, K.; Grätzel, M. Hydrophobic, Highly Conductive Ambient-Temperature Molten Salts. *Inorg. Chem.* **1996**, *35*, 1168–1178, Correction: *Inorg. Chem.* **1998**, *37*, 166.
- Riddick, J. A.; Bunger, W. B.; Sakano, T. K. *Organic Solvents: Physical Properties and Methods of Purification*, 4th ed.; John Wiley & Sons: New York, 1986.
- Christensen, C.; Gmehling, J.; Rasmussen, P.; Weidlich, U., Eds. *Heats of Mixing Data Collection, DECHEMA Chemistry Data Series*; Schön & Wetzel GmbH: Frankfurt/Main, F. R. Germany, 1984–1991.
- Marsh, K. N., Ed. *Recommended Reference Materials for the Realization of Physicochemical Properties*; Blackwell Scientific Publications: Oxford, 1987.
- Domańska, U.; Marciniak, A. Activity Coefficients at Infinite Dilution Measurements for Organics Solutes and Water in the Ionic Liquid

- 1-Ethyl-3-methylimidazolium Trifluoroacetate. *J. Phys. Chem. B* **2007**, *111*, 11984–11988.
- (42) Domaille, P. J.; Druliner, J. D.; Gosser, L. W.; Read, J. M.; Schmelzer, E. R.; Stevens, W. R. Triphenylborane Methanolysis and Equilibrium Association between Triphenylborane or Diphenylborinate Esters and Alcohols. *J. Org. Chem.* **1985**, *50*, 189–194.
- (43) *Solaris, Advanced Chemistry Development (ACD/Labs) Software V8.14*, 1994–2007.
- (44) Lide, D. R., Ed. *CRC Handbook of Chemistry and Physics*, 84th ed.; CRC Press LLC.: Boca Raton, 2003.
- (45) Benninga, H. *A history of lactic acid making*; Kluwer Academic Publishers: The Netherlands, 1990.

Received for review April 9, 2008. Accepted June 7, 2008. We acknowledge the Department of Energy (grant DOE FG02-05CH11294) for funding.

JE800248W